

Targeting Apoptosis via Chemical Design: Inhibition of Bid-Induced Cell Death by Small Organic Molecules

Barbara Becattini, Sina Sareth,¹ Dayong Zhai,¹ Kevin J. Crowell, Marilisa Leone, John C. Reed, and Maurizio Pellecchia*
The Burnham Institute
10901 North Torrey Pines Road
La Jolla, California 92037

Summary

Bid is a key member of the Bcl-2 family proteins involved in the control of the apoptotic cascade in cells, leading to cell death. Uncontrolled cell death is associated with several human pathologies, such as neurodegenerative diseases and ischemic injuries. Therefore, Bid represents a potential yet unexplored and challenging target for strategies aimed at the development of therapeutic agents. Here we show that a multidisciplinary NMR-based approach that we named SAR by ILOEs (structure activity relationships by *interligand nuclear Overhauser effect*) allowed us to rationally design a series of 4-phenylsulfanyl-phenylamine derivatives that are capable of occupying a deep hydrophobic crevice on the surface of Bid. These compounds represent the first antiapoptotic small molecules targeting a Bcl-2 protein as shown by their ability to inhibit tBid-induced SMAC release, caspase-3 activation, and cell death.

Introduction

Apoptosis is a crucial process for tissue homeostasis that is controlled by the Bcl-2 family proteins, which includes anti- and proapoptotic members [1–3]. Among the proapoptotic proteins of this family are Bax-like proteins, whose amino acid sequences show a high degree of similarity to the antiapoptotic family members, and BH3-only proteins, whose similarity to the Bcl-2 members is limited to the BH3 region, a dimerizing motif shared by essentially all family members [4]. Bid is a widely expressed member of the BH3-only proteins consisting of 195 amino acid residues whose active form is believed to be the 15 kDa N-truncated derivative (tBid) that results from caspase-8 cleavage of the full-length 22 kDa protein [5, 6]. Caspase-8-mediated cleavage at the Bid N-terminal region not only exposes the BH3 domain but also results in myristoylation of tBid, thus prompting tBid to translocate from the cytosol to mitochondrial membranes where it integrates [7]. Once at the outer mitochondrial membrane tBid interacts with multidomain proapoptotic proteins Bax and Bak, inducing their oligomerization in membranes of mitochondria and triggering changes in mitochondrial membrane permeability, which result in release of apoptogenic pro-

teins such as cytochrome c and SMAC/DIABLO [8–10] (Figure 1A).

The generation of Bid knockout mice has begun to reveal the pathophysiological roles of this proapoptotic protein in vivo. These mice are viable, lacking developmental abnormalities. However Bid^{-/-} mice are resistant to hepatic cell apoptosis and liver injury when injected with antibodies directed against TNF-family death receptor Fas [11]. Mice lacking Bid also display resistance to brain injury in a stroke model involving transient middle cerebral artery occlusion [12]. In addition, recent studies using transgenic mice models of amyotrophic lateral sclerosis (ALS) strongly suggest a pivotal role for Bid in the overall cascade of molecular events responsible for the onset and progression of this neurodegenerative process [13]. Taken together, these results show that Bid is a key molecule in the control of apoptosis in vivo and suggest that it could be a molecular target for treatment of pathologies associated with uncontrolled cell death.

While several small molecule inhibitors of antiapoptotic members of the Bcl-2 family have been reported [14–22], so far no inhibitors have been discovered against the proapoptotic members including Bid. Antagonists of antiapoptotic proteins Bcl-2 and Bcl-X_L have been based on targeting the site on these proteins responsible for binding BH3 peptides [14–19]. However, an analogous strategy cannot be applied to Bid, as the molecular basis for its function have not yet been characterized. The three-dimensional structure of mouse Bid, as elucidated by NMR spectroscopy [7, 23], reveals the presence of a deep hydrophobic crevice on the surface of the protein in a region that is conserved between mouse and human Bid, just adjacent to the BH3 peptide region. Taking advantage of a combined approach involving an NMR fragment-based screening, *interligand nuclear Overhauser effect* (ILOEs), molecular modeling, and synthetic chemistry, we obtained compound BI-6C9 that is capable of binding into this crevice. We show here that this binding results in loss of proapoptotic activity of Bid in vitro and in cells (Figure 1B). The data obtained clearly demonstrate the ability of our approach that we named SAR by ILOEs (structure activity relationships by *interligand nuclear Overhauser effect*), to tackle challenging drug targets such as those involving protein-protein interactions.

Results

Strategy

To design small molecule compounds capable of occupying the deep hydrophobic crevice on the surface of Bid, we adopted a fragment-based approach. A tighter chemical binder is built from pairs of compounds that bind to adjacent sites on Bid, using a small but diverse library of molecular fragments [24, 25]. This library includes low molecular weight compounds (MW <300) that represent a selection of the substructures fre-

*Correspondence: mpellecchia@burnham.org

¹These authors contributed equally to this work.

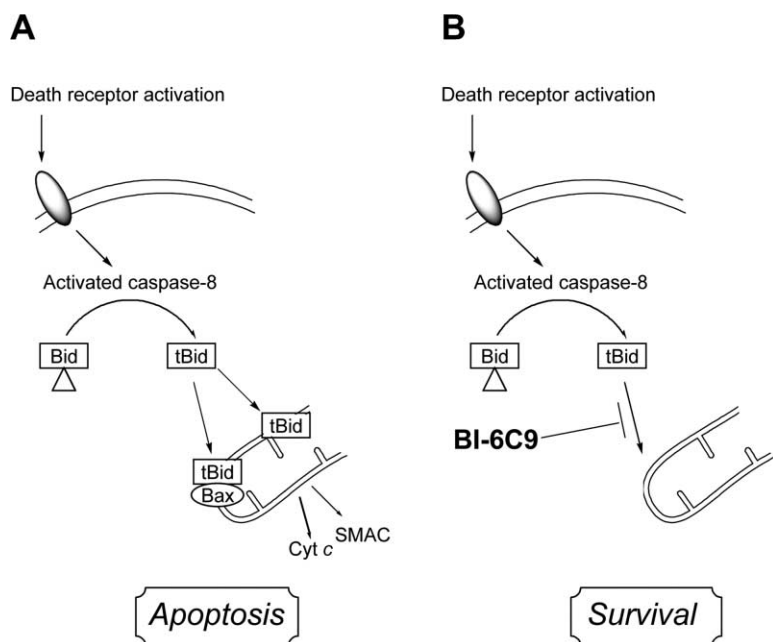


Figure 1. Bid-Induced Cell Death

(A) Apoptosis induced by caspase-8 mediated Bid activation.

(B) Compounds capable of blocking tBid migration would result in cell survival.

quently found in drugs [26] and that are amenable to subsequent chemistry. Because the compounds have very simple structures, a library of a few hundred derivatives is typically sufficient to represent the diverse frameworks. However, due to their limited size and consequent limited number of possible interactions with a given protein, a few of the small fragments will exhibit at most low affinity for the target. For this reason, we applied solution nuclear magnetic resonance (NMR) spectroscopy as screening method, since it allows the detection of very weak binders [27].

A valuable NMR-based technique to screen a library of compounds and validate their binding to a target protein is the measurement of transferred NOEs [24, 28, 29]. Since small molecules tumble rapidly in solution, the dominant ^1H relaxation mechanisms during a NOESY-type experiment lead to weak, positive NOEs (crosspeaks have opposite sign than diagonal peaks). On the contrary, when the ligand is bound even transiently to a target protein it assumes its long correlation time. In the case of a rapid exchange between free and bound state (namely when $k_{\text{off}} \gg 1/T_1$, the longitudinal relaxation rate), this translates into very strong negative NOEs (i.e., very strong positive crosspeaks in a NOESY-type experiment). The use of 2D [^1H , ^1H]-NOESY spectra [30] is then obvious in the search for small molecular binders. In a mixture of compounds in presence of a substoichiometric amount of target (Bid), only those compounds that bind appreciably to the protein will exhibit strong negative NOEs, whereas nonbinders will show no NOEs or at most very weak positive ones. In addition, if two or more ligands bind simultaneously in adjacent sites on the protein surface, strong negative ligand-ligand NOEs (ILOEs) can also be observed [31–35]. Compounds that display ligand-ligand interactions can then serve to design covalently linked compounds with increased affinity [31–35]. We demonstrate here that the detection of such interactions can be accom-

plished also in complex mixtures, where deconvolution can be easily achieved aided by the NMR spectra of individual compounds.

We prepared several mixtures of compounds from our library of scaffolds (0.4–0.9 mM each) and tested them in presence of 10 μM Bid (Figure 2A). Typical trNOESY spectra were measured with 8 or 16 transients per increment with mixing times of 300–800 ms, to maximize the detection of trNOEs and ILOEs [32]. Pooling compounds in mixtures of 6–24 allowed the collection of the spectra for our 300 fragments library in a few days. Analysis of the data and subsequent deconvolution of the spectra allowed us to identify weak ligands by means of positive trNOEs crosspeaks. Similarly, compounds that bind Bid in close proximity (less than 5 Å) are identified by detecting intermolecular NOEs (ILOEs) [31–35] serving as building blocks for producing linked compounds. As depicted in Figures 2B and 2C, the experiments were repeated for the pairs that were recognized to bind to Bid, such as BI-2A1/BI-2A7 (Figure 2B) and BI-2A2/BI-2A7 (Figure 2C).

To identify the amino acids involved in this interaction, we prepared ^{15}N -labeled Bid and acquired 2D [^{15}N , ^1H]-TROSY spectra in absence and presence of the weak binders [33, 36] (Figure 3A). As a result of the addition of BI-2A7 to ^{15}N -labeled Bid, several modifications resulted in the [^{15}N , ^1H]-TROSY spectrum of the protein and analysis of the chemical shift perturbations, based on the published resonance's assignments [7], allowed us to map the interactions with the ligand. The residues mostly affected by this binding were S28, A87, L105, A137, G143, N144, K146, F171, L182, T185, and S184. The changes were plotted on the three-dimensional structure of Bid and showed that most of the changes fall in proximity of the deep hydrophobic groove on the surface of the protein (Figure 3B, red areas).

Once the interaction sites on the Bid surface were identified by chemical shift mapping, we docked the

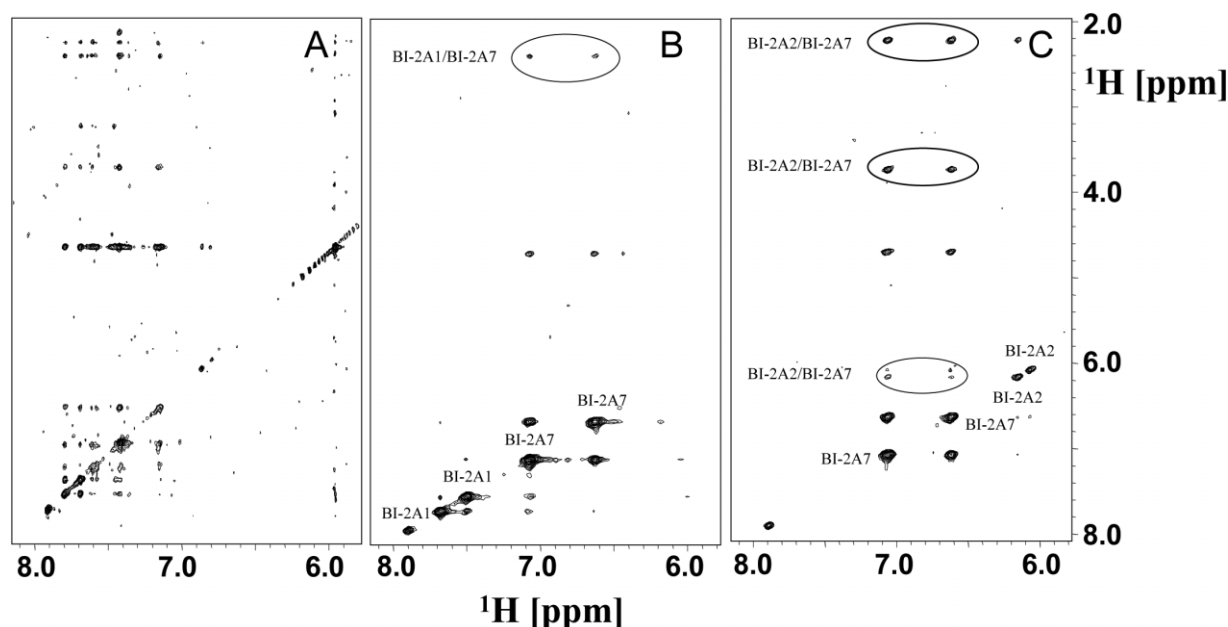


Figure 2. Intra- and Interligand-Based Identification of Small Compounds that Bind BID

(A) Spectrum of a mixture of 12 small molecules (0.4–0.9 mM each) in presence of Bid (10 μ M), with many NOE crosspeaks present.

(B) Spectrum of a solution of BI-2A1 and BI-2A7 in presence of Bid (10 μ M).

(C) Spectrum of a solution of BI-2A2 and BI-2A7 in the presence of Bid (10 μ M). In (B) and (C) ILOE crosspeaks between the two molecules are circled.

two pairs of building blocks in the three-dimensional structure of the protein to envisage possible linkers between the two fragments. We focused initially on the pair BI-2A1/BI-2A7 since the resulting compounds were synthetically more accessible. To prioritize the synthetic efforts, we relied heavily on *in silico* docking by using FlexX [37] as implemented in Sybyl (TRIPOS, Inc.) followed by CSCORE analysis and visual inspection. We docked several compounds and the chemical structures of eight of them are reported in Table 1 (first column) together with the fragments BI-2A2, BI-2A1, and BI-2A7. The best results in terms of fitting in the hydrophobic groove were observed for BI-6C8 and BI-6C9 (Figure 4A), whereas the corresponding 5-carbons linker derivatives did not dock well. Therefore, by using a combination of mixture-based trNOEs and ILOEs screening (SAR by ILOEs), chemical shift mapping, and virtual docking, we designed a first series of bi-dentate compounds targeting the hydrophobic groove near the BH3 region of Bid (Figure 4B).

Synthesis and Binding Studies

The combined NMR and virtual docking approach resulted in the design of compounds BI-6C8 and BI-6C9 as potential Bid antagonists. Nonetheless, we decided to synthesize and evaluate the binding properties of other derivatives to verify the validity of our approach. The synthesis of eight 4-phenylsulfanyl-phenylamine derivatives is described in Figure 5A. Peptide bond formation was aided by resin-bound carbodiimide, such as *N*-cyclohexylcarbodiimide-*N'*-propylmethyl polystyrene (PS-CDI) (Argonaut Technologies) or 1-ethyl-3-(3-dimethylaminopropyl)carbodiimide hydrochloride (WS-

CDI) [38], using as starting materials the commercially available 4-amino-4'-nitrodiphenyl sulfide and the *N*-Boc amino acid ($n = 3$ or $n = 5$). Stirring the reaction mixture at room temperature resulted in the corresponding Boc-protected amines BI-6C6 and BI-6C12. Deprotection with trifluoroacetic acid (TFA) gave the free amines BI-6C7 and BI-6D1 in good yields (Figure 5A). Following reaction with 4-methoxybenzenesulfonyl chloride afforded the corresponding sulfonamides BI-6C8 and BI-6D2 in very high yields. The synthesis was completed by reducing the aromatic nitro group to the amines BI-6C9 and BI-6D3 in presence of tin dichloride (SnCl_2) [39].

To examine the binding affinity of these bi-dentate derivatives to Bid, we measured 2D [^{13}C , ^1H]-HSQC spectra in presence of ^{13}C methionine-labeled protein, as at least one methionine is present in the hydrophobic groove of Bid (Figure 4B). As described earlier, we initially evaluated the binding affinity of these compounds from chemical shifts induced upon titration. The results are reported in Table 1 (column 2) and are qualitatively in good agreement with the predictions based on virtual docking studies. Figure 5C shows the 2D [^{13}C , ^1H]-HSQC spectrum of ^{13}C methionine-labeled Bid upon addition of BI-6C9. The binding of BI-6C9 appears to be slow on the NMR timescale, as indicated by the appearance/disappearance of crosspeaks in the spectrum upon titration (Figure 5C). Monitoring the variation of crosspeak intensity upon addition of increasing amounts of BI-6C9, allowed us to estimate its dissociation constant ($K_D \sim 20 \mu\text{M}$, Figure 5D).

To further confirm the binding of BI-6C9 into the crevice on the surface of Bid, we also performed $T_{1\rho}$ competition experiments. In these experiments, the relaxation

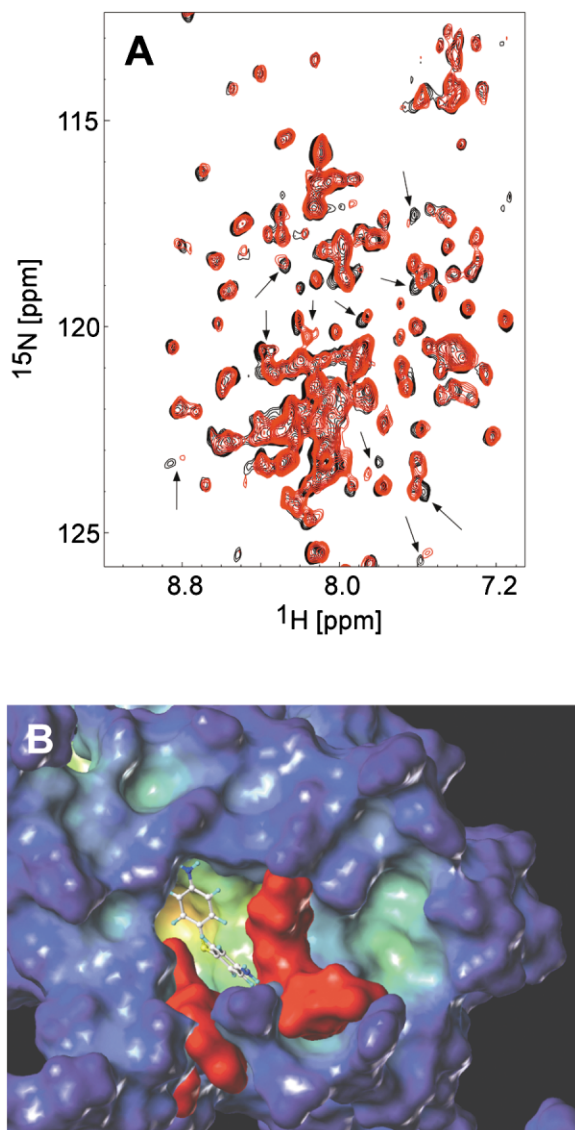


Figure 3. Chemical Shift Mapping

(A) 2D [^{15}N , ^1H]-TROSY spectrum measured with a sample of 0.5 mM BID in the absence (black) and presence (red) of 1 mM BI-2A7. Arrows indicate those resonances that are affected by the presence of BI-2A7.

(B) Chemical-shift mapping and docking of BI-2A7 into the three-dimensional structure of Bid (PDB code 1DDDB). Regions affected by the binding of BI-2A7 are highlighted in red. This and all other figures showing the surface of Bid were generated by MOLCAD [49]. The color code is according to cavity depth: blue, shallow; yellow, deep.

effects detected on the ^1H signals of compound BI-2A7 induced by the presence of Bid (10 μM) are competed with small amounts of BI-6C9 (10 μM) (data not shown).

Finally, we also performed chemical shift mapping using BI-6C9 and ^{15}N -Bid. Although the shifts are not very large, presumably due to the limited solubility of the compound at the concentrations (high micromolar) needed for such experiments or because the complex may be in the slow to intermediate exchange with respect to ^1H and ^{15}N resonances, larger and more evident

effects were obtained with ^{15}N -Bid after cleavage with caspase-8, leading to tBid [5, 6]. This observation suggests that the truncated Bid protein is capable of binding even better to our compound than full-length Bid.

In Vitro and Cell-Based Assays

We tested the two fragments and all the newly synthesized compounds in vitro for their ability to inhibit Bid-mediated release of SMAC using mitochondria isolated from HeLa cells. Each compound was tested at a concentration of 50 μM . As illustrated in Figure 6A, only BI-6C9 was able to significantly reduce tBid-induced SMAC release at this concentration. This compound was then tested at several doses using the same mitochondria-based assay, showing that it dramatically decreased SMAC release at concentrations as low as 20 μM (Figure 6B). To preliminarily investigate the mechanism by which BI-6C9 reduces SMAC release from isolated mitochondria, we tested its effects on association of recombinant tBid protein with mitochondria in vitro. Accordingly, the tBid protein was treated with different concentrations of BI-6C9, after which it was incubated with mitochondria, followed by analysis of the bound and unbound fractions by immunoblotting using Bid antibody. The concentration of mitochondria-bound tBid diminished in response to increasing concentrations of BI-6C9. Dose-response experiments showed that the compound is effective at inhibiting tBid association with isolated mitochondria at 20 μM (Figure 6C).

BI-6C9 was also evaluated for its ability to inhibit Bid-induced apoptosis in cell. For these experiments, HeLa cells were transfected with a plasmid encoding tBid, and effector caspase activity was measured in cell lysates 24 hr later. BI-6C9 reduced caspase-3 activity in tBid-transfected cells by ~ 4 -fold at 50 μM , whereas caspase activity was totally blocked at 100 μM (Figure 6D). Moreover, tBid-induced cell death, as measured by caspase-3 activity, was reduced from $80\% \pm 5\%$ to $35\% \pm 5\%$ by 50 μM BI-6C9 (Figure 6E).

As controls we verified that BI-6C9 does not bind appreciably to other Bcl-2 family proteins such as Bcl-X_L (NMR binding assay).

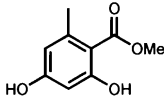
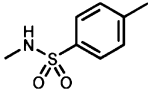
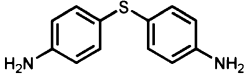
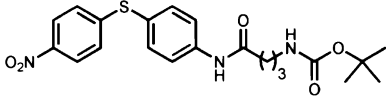
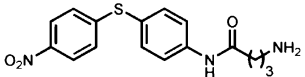
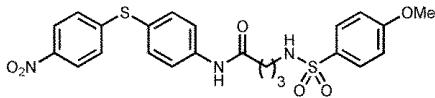
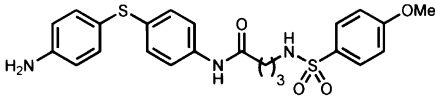
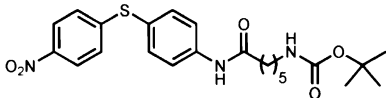
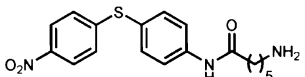
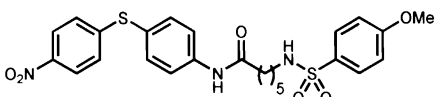
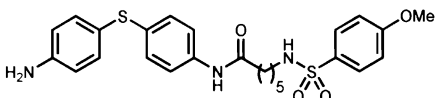
Finally, we have also determined that our compound does not impair caspase-8-mediated Bid cleavage (by SDS page) and does not inhibit caspase-3 (in vitro assay) at the concentrations used in the cellular assay (data not shown).

Discussion

Several evidences show that Bid plays a central role in the apoptotic machinery mediating cytochrome c and SMAC/DIABLO release from mitochondria, a crucial event for caspase activation and cell death [40] (Figure 1). Pharmacological inhibition of Bid could therefore provide a protective benefit against pathological cell death, occurring in cerebral ischemia, neurodegenerative diseases, liver inflammation, or other illnesses where Bid has been implicated [12, 13, 41, 42].

By screening of a small library of compounds using NMR, we isolated pairs of molecules that bind to adjacent sites on Bid. Aided by computational modeling,

Table 1. Chemical Structures and Assay Data

Compound	Structure	Fitting in the Two Subpockets	NMR Binding	SMAC Release Inhibition at 50 μ M (%)
BI-2A2		ND	— ^a	ND
BI-2A1		ND	— ^a	0
BI-2A7		+	+	22
BI-6C6		++	++	14
BI-6C7		++	+	66
BI-6C8		++++	+++	24
BI-6C9		+++	++++	100
BI-6C12		++	ND	0
BI-6D1		++	ND	60
BI-6D2		—	—	16
BI-6D3		—	ND	ND

Qualitative data in terms of docking (fitting in the two subpockets, column 1), chemical shifts in HSQC spectra (NMR, column 2), and in vitro assays on isolated mitochondria (SMAC release inhibition, column 3) for the two fragments (BI-2A1 and BI-2A7) and the eight newly synthesized compounds. Results are represented by plus and minus or by percentage of inhibition of SMAC release. ND, not determined.

^aiLOEs with BI-2A7 were observed.

we identified possible linkers for covalently binding the pairs of compounds, thus arriving at high affinity binders. Note that, as anticipated by Fejzo et al. [24], Li et al. [32], and Kline [35], the fragment-based approach of linking binders detected via trNOEs and iLOEs is of

general applicability and does not necessarily require the knowledge of the three-dimensional structure or the availability of isotopically (¹⁵N and/or ¹³C and/or ²H) labeled target. One could simply synthesize compounds with linkers of different length and nature and test the

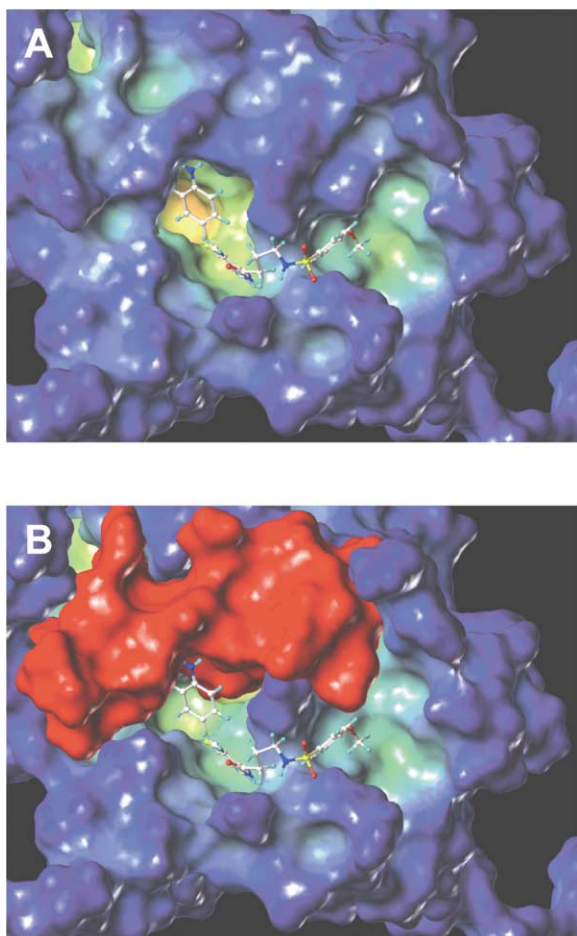


Figure 4. Virtual Docking of BI-6C9 into the Three-Dimensional Structure of Bid

(A) BI-6C9 sits in the hydrophobic groove.

(B) The hydrophobic groove is near to the BH3 peptide which is highlighted in red.

resulting compounds for binding and activity. Analysis of trNOEs and ILOEs build-up rates can also provide some structural information on the relative orientation of the two fragments [32, 43]. However, for a successful implementation of this strategy, the library must be carefully designed to optimize the detection of ligand-ligand interactions by selecting compounds with appropriate derivatizations of functional groups with proton NMR-detectable substituents. Furthermore, the introduction of heteroatoms in these substituents also results in large chemical shift dispersion between the compounds of the library, thus enabling the detection of ILOEs in complex mixtures, as we reported here. For example, in compound BI-2A1 (Table 1) the benzenesulfonic acid is derivatized with a methylamine group. This enables on the one hand the observation of trNOEs and ILOEs to its methyl group and on the other it provides a scaffold that chemically resembles more closely the bi-dentate compound. Should one have used benzenesulfonic acid instead, not only the negative charge could have influenced the binding but the detection of trNOEs and, most importantly, ILOEs, would have been limited by the ab-

sence of observable protons close to the sulfonic acid group. In summary, while the use of ILOEs in the design of bi-dentate compounds or to improve an existing lead is an attractive application for drug discovery [21, 29], we demonstrate here that a key element for the successful implementation of such strategy is the optimal design of the scaffold library for the detection of such interactions by NMR.

As shown, our method (SAR by ILOEs) can be combined with chemical shift mapping in the three-dimensional structure of the protein target (if available) and molecular modeling in the design of bi-dentate compounds. Again, this is not an indispensable step, but it can result in a reduced number of molecules to be synthesized and tested.

Among the eight synthesized compounds, BI-6C9 was found to be the strongest Bid binder, and *in vitro* it dramatically reduced tBid-induced release of SMAC from isolated mitochondria at concentrations as low as 20 μ M (Figure 6B). Moreover, cell-based assays showed that this compound effectively inhibits tBid-mediated caspase activation and cell death already at concentrations as low as 50 μ M.

The precise mechanism by which this compound inhibits the activity of Bid remains to be determined. Several evidences support a role for the BH3 peptide region of Bid as a critical effector of apoptosis, which binds Bax and Bak, activating these proapoptotic proteins to affect changes in mitochondrial membrane permeability [44–46]. However, Bid is also capable of inserting in membranes, possibly functioning as an ion channel [47]. We speculate here that occupancy of the hydrophobic crevice of Bid or tBid by our compound either interferes with exposure of the BH3 domain or blocks insertion of tBid in membranes by maintaining Bid in an inactive conformation.

In conclusion, we have successfully utilized a combination of NMR and virtual docking approaches to discover a small bi-dentate molecule capable of inhibiting Bid *in vitro* and in cells. This compound could be useful in deciphering the complex mechanism of action and cellular functions of Bid in apoptosis. Further optimization of BI-6C9 might result in compounds with improved affinity for Bid and favorable pharmaceutical properties that permit its testing in animal models of diseases, thus providing a starting point for development of potential drug candidates for human illnesses associated with uncontrolled cell death.

Significance

We have demonstrated that a multidisciplinary approach (SAR by ILOE) taking advantage of NMR-based fragment screening, molecular modeling, and synthetic chemistry allowed us to rationally design a series of 4-phenylsulfanyl-phenylamine derivatives that are capable of occupying a deep hydrophobic crevice on the surface of Bid. We have also demonstrated that this binding results in inhibition of tBid-induced SMAC release, caspase-3 activation, and cell death. As such, our compounds could be useful in deciphering the complex mechanism of action and cellular functions

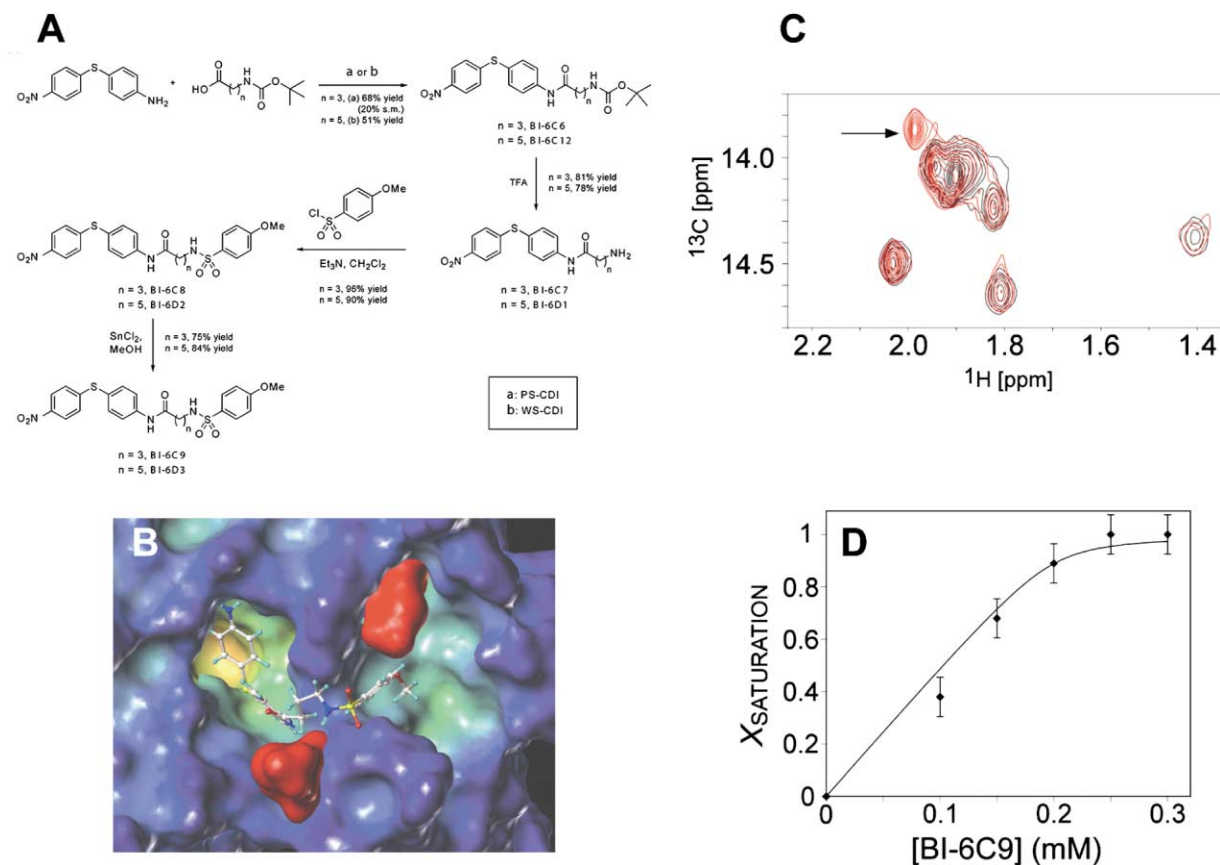


Figure 5. Chemical Synthesis, Virtual Docking of BI-6C9, and NMR Characterization of K_d
 (A) Synthetic scheme for the bi-dentate ligands with 3- and 5-carbons linker.
 (B) Docking of BI-6C9 into the three-dimensional structure of Bid. In red are highlighted the two methionines present in the hydrophobic groove.
 (C) 2D [^1H , ^{13}C]-HSQC of $^{\gamma}\text{-}^{13}\text{C}$ -Met Bid (200 μM) in the absence (black) and presence (red) of 150 μM BI-6C9. The arrow indicates the peak that was monitored to determine the K_d for BI-6C9.
 (D) Plot of the peak volume versus the concentration of BI-6C9. The peak volume was referenced to a peak that was unaffected by BI-6C9, and the peak volume was plotted as the fraction of the maximum peak volume observed for saturation of Bid with BI-6C9.

of Bid in the apoptotic cascade and provide a valuable starting point for development of potential drug candidates for human illnesses associated with uncontrolled cell death. Furthermore, the data obtained clearly demonstrate the ability of the SAR by ILOE approach to tackle challenging drug targets. We anticipate that possible future applications could include the design of potential antagonists of protein-protein and protein-nucleic acids interactions.

Experimental Procedures

Library Design

The NMR compound library is composed by ~ 300 low molecular weight compounds representing diverse core structures. This library was assembled and individual 1D ^1H spectra were measured in D_2O buffer as control of compound purity, stability, and solubility in water buffer. In designing the NMR library, particular emphasis was put into the chemical properties of the selected compounds in an attempt to address “drug likeness” on empirical grounds. In this respect, compounds with reactive functional groups such as halides, anhydrides, epoxides, aziridines, phosphonate and sulphonate esters, imines, aldehydes, Michael acceptors, and halopyrimidines, were not included. The compounds were also selected in view of

their subsequent use as building blocks for the synthesis of bi-dentate compounds, eliminating fragments that would lead to tethered ligands with undesirable critical properties. The following criteria were adopted: average molecular weight < 300 , octanol/water repartition coefficient (LogP) < 1.3 , and number of rotatable bonds between 0 and 2. The goal in using these empirical drug-like property filters is to predict favorable outcome in ADME (adsorption, distribution, metabolism, excretion) studies, as well as final success as drug in humans. In addition, availability of each fragment in larger amounts at low cost as well as ease of synthesis and conversion to more complex structures, were also taken into consideration in selecting the scaffolds. Finally, our library was designed to optimize the detection of trNOEs and ILOEs by selecting compounds with appropriate derivatization of functional groups with proton NMR-detectable substituents.

Protein Expression and Purification

Recombinant full-length mouse Bid was produced from a pET-19b (Novagen) plasmid construct containing the entire nucleotide sequence for Bid fused to an N-terminal poly-His tag. Unlabeled Bid was expressed in *E. coli* BL21 in LB media at 37°C, with an induction period of 3–4 hr with 1 mM IPTG. ^{15}N -labeled Bid was similarly produced, with growth occurring in M9 media supplemented with 0.5 g/l $^{15}\text{NH}_4\text{Cl}$. $\epsilon\text{-}^{13}\text{C}$ -Met-labeled Bid was produced in M9 media supplemented with 50 mg/l of $\epsilon\text{-}^{13}\text{C}$ -Met at time of induction with

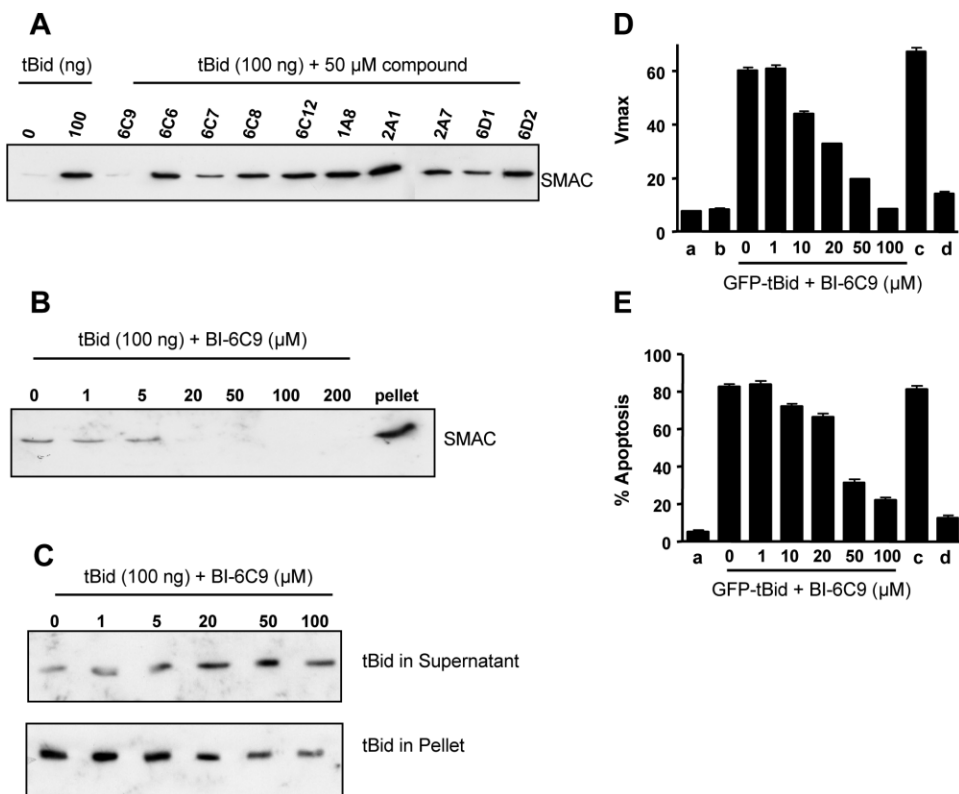


Figure 6. Suppression of tBid Activity In Vitro and in Cells by Bid Binding Compounds

(A) Effect of compounds on SMAC release from mitochondria isolated from HeLa cells. The first lane represents mitochondria incubated without tBid. All others received 100 ng tBid without or with compounds.

(B) BI-6C9 blocks tBid-induced SMAC release from mitochondria isolated from HeLa cells.

(C) BI-6C9 blocks tBid association with mitochondria.

(D and E) BI-6C9 reduces tBid-induced caspase activation in 293T cells (D). BI-6C9 reduces tBid-induced cell death in 293T cells (E). a, GFP; b, GFP + BI-6C9 100 μ M; c, GFP + BI-6C8 100 μ M; d, Z-VAD-fmk.

IPtG. Following cell lysis, soluble Bid was purified over a Hi-Trap chelating column (Amersham, Pharmacia), followed by ion-exchange purification with a MonoQ (Amersham, Pharmacia) column. Final Bid samples were dialyzed into a buffer appropriate for the subsequent experiments. tBid was produced by cleavage of purified Bid with caspase-8, as reported [47].

Molecular Modeling

Molecular modeling studies were conducted on several R12000 SGI Octane workstations with the software package Sybyl version 6.9 (TRIPOS). The docked structures of the compounds were initially obtained by FlexX [37] as implemented in Sybyl. Molecular models of compounds were energy minimized with MAXIMN2 (Sybyl). For each molecule, 20 solutions were generated and ranked according to CSCORE [48]. The solutions were finally ranked by visual inspection of the linked compounds in the deep hydrophobic groove on the surface of Bid. Surface representations were generated by MOLCAD [49].

NMR Spectroscopy

For all NMR experiments, Bid was exchanged into 50 mM phosphate buffer at pH 7.5 and measurements were performed at 30°C. 2D [15 N, 1 H]-TROSY spectra for Bid were measured with 0.5 mM samples of 15 N-labeled Bid. 2D [13 C, 1 H]-HSQC spectra were measured with 0.2 mM samples of ϵ - 13 C-Met-labeled Bid. 2D [1 H, 1 H]-NOESY spectra were acquired with small molecules at a concentration of 0.9 mM in the presence of 10 μ M BID. $T_{1\rho}$ competition experiments (200 ms spin-lock duration) were performed on either 100 μ M BI-2A7 or a mixture of 100 μ M BI-2A7 and 10 μ M BI-6C9, in the presence and absence of 10 μ M Bid. All experiments were performed with either

a 500 or 600 MHz Bruker Avance spectrometer, both equipped with TXI probes. Typical parameters for the 2D [15 N, 1 H]-TROSY spectra included 1 H and 15 N $\pi/2$ pulse lengths of 11 and 40 μ s, respectively; 1 H and 15 N sweep widths of 12 and 32 ppm, respectively; 16 scans and 256 indirect acquisition points; and a recycle delay of 1 s. For the 2D [13 C, 1 H]-HSQC typical parameters included 1 H and 13 C $\pi/2$ pulse lengths of 10 and 13 μ s, respectively; 1 H and 13 C sweep widths of 12 and 5 ppm, respectively; 128 scans and 80 indirect acquisition points; and a recycle delay of 1 s. 2D [1 H, 1 H]-NOESY spectra were typically acquired with eight scans for each of 400 indirect points, a 1 H $\pi/2$ pulse length of 11 μ s, sweep widths of 12 ppm in both dimensions, mixing times of 300–800 ms, and a recycle delay of 1 s. In all experiments, dephasing of residual water signals was obtained with a WATERGATE sequence.

Chemistry

{3-[4-(4-Nitro-Phenylsulfanyl)-Phenylcarbamoyl]-Propyl}-Carbamic Acid Tert-Butyl Ester (BI-6C6)

N-Cyclohexylcarbodiimide-*N'*-propylmethyl polystyrene (PS-CDI resin, 730 mg, 1.0 mmol) was added to a dry, round-bottomed flask. *t*-Boc-4-aminobutanoic acid (152 mg, 0.75 mmol) was added as a solution in CH_2Cl_2 (4 ml) and the reaction mixture was stirred at room temperature. After 5 min, 4-amino-4'-nitrodiphenyl sulfide (123 mg, 0.5 mmol) in 4 ml of CH_2Cl_2 was added and the suspension stirred at room temperature for 4 days. The reaction mixture was filtered under vacuum and the resin was washed twice with CH_2Cl_2 . Concentration of the filtrate afforded a crude that was purified by flash chromatography (hexane/ethyl acetate 1:1) to give the pure BI-6C6 (274 mg, 64%) as a yellow solid, together with unreacted starting

material (25 mg, 20%). ¹H NMR (*d*-DMSO, 500 MHz): 10.19 (s, 1H), 8.13 (d, *J* = 8.5 Hz, 2H), 7.78 (d, *J* = 8.5 Hz, 2H), 7.55 (d, *J* = 8.5 Hz, 2H), 7.23 (d, *J* = 8.5 Hz, 2H), 3.00–2.97 (m, 2H), 2.37–2.34 (m, 2H), 1.73–1.70 (m, 2H), 1.39 (s, 9H). ¹³C NMR (*d*-DMSO, 125 MHz): 171.3, 155.6, 148.8, 144.7, 141.0, 135.9, 125.9, 124.2, 123.1, 121.7, 77.4, 33.8, 29.2, 28.2, 27.1.

4-Amino-N-[4-(4-Nitro-Phenylsulfanyl)-Phenyl]-Butyramide (BI-6C7)

Compound BI-6C6 (274 mg, 0.63 mmol) was added to a round-bottomed flask and cooled to 0°C. The minimum amount of trifluoroacetic acid needed to dissolve the compound was added and the solution stirred at room temperature for an additional 5 min. The acid was evaporated using a rotary evaporator and the residue dissolved in CH₂Cl₂. The solution was extracted with a 1 M solution of K₂CO₃ and water. The organic phase was dried over Na₂SO₄ and concentrated under reduced pressure to give the crude BI-6C7 (170 mg, 81%) as a bright yellow solid. The compound was used with no further purification. ¹H NMR (*d*-DMSO, 500 MHz): 8.13 (d, *J* = 6.0 Hz, 2H), 7.78 (d, *J* = 9.5 Hz, 2H), 7.55 (d, *J* = 6.0 Hz, 2H), 7.23 (d, *J* = 9.5 Hz, 2H), 2.61–2.58 (m, 2H), 2.40–2.39 (m, 2H), 1.70–1.67 (m, 2H). ¹³C NMR (*d*-DMSO, 125 MHz): 171.9, 148.8, 144.7, 141.1, 135.9, 125.8, 124.2, 123.1, 121.7, 41.1, 34.1, 29.0.

4-(4-Methoxy-Benzenesulfonylamino)-N-[4-(4-Nitro-Phenylsulfanyl)-Phenyl]-Butyramide (BI-6C8)

A suspension of the amine BI-6C7 (33 mg, 0.1 mmol) and triethylamine (13 mg, 0.13 mmol) in 1 ml of CH₂Cl₂ was cooled to 0°C and 4-methoxybenzoyl chloride (23 mg, 0.11 mmol) was added as a solution in 1.5 ml of CH₂Cl₂. After stirring 2 hr at 0°C and overnight at room temperature, the reaction mixture was washed with water and a saturated solution of NaCl in water. The organic phase was dried over Na₂SO₄ and concentrated under reduced pressure to afford BI-6C8 (48 mg, 96%) as a light yellow solid. ¹H NMR (*d*-DMSO, 500 MHz): 10.18 (s, 1H), 8.13 (d, *J* = 9.0 Hz, 2H), 7.77–7.72 (m, 4H), 7.55 (d, *J* = 8.5 Hz, 2H), 7.50 (t, *J* = 6.0 Hz, 1H), 7.23 (d, *J* = 9.0 Hz, 2H), 7.11 (d, *J* = 8.5 Hz, 2H), 3.84 (s, 3H), 2.78–2.74 (m, 2H), 2.40–2.38 (m, 2H), 1.74–1.69 (m, 2H). ¹³C NMR (*d*-DMSO, 125 MHz): 171.0, 162.0, 159.6, 159.5, 159.3, 157.5, 148.8, 140.9, 132.0, 125.9, 124.2, 121.8, 114.2, 55.5, 41.9, 36.7, 32.0.

N-[4-(4-Amino-Phenylsulfanyl)-Phenyl]-4-(4-Methoxy-Benzenesulfonylamino)-Butyramide (BI-6C9)

To a suspension of BI-6C8 (38 mg, 0.077 mmol) in 2 ml of MeOH was added SnCl₂ (85 mg, 0.38 mmol) and the mixture was refluxed for 5 hr. Methanol was then evaporated and a solution 10% NaHCO₃ was added carefully at 0°C. The residue was extracted with ethyl acetate and the combined organic phases were dried over Na₂SO₄ and concentrated under reduced pressure to give BI-6C9 (27 mg, 75%) as a dark yellow solid. ¹H NMR (*d*-DMSO, 500 MHz): 9.84 (s, 1H), 7.70 (d, *J* = 9.0 Hz, 2H), 7.46–7.43 (m, 3H), 7.13–7.07 (m, 4H), 7.01 (d, *J* = 8.5 Hz, 2H), 6.58 (d, *J* = 9.0 Hz, 2H), 3.81 (s, 3H), 2.73–2.69 (m, 2H), 2.29–2.26 (m, 2H), 1.67–1.63 (m, 2H). ¹³C NMR (*d*-DMSO, 125 MHz): 170.4, 161.9, 149.4, 137.0, 135.3, 132.7, 131.9, 128.5, 127.8, 119.7, 116.4, 114.7, 114.2, 55.5, 42.0, 33.2, 24.8.

{5-[4-(4-Nitro-Phenylsulfanyl)-Phenylcarbamoyl]-Pentyl}-Carbamic Acid Tert-Butyl Ester (BI-6C12)

1-ethyl-3-(3-dimethylaminopropyl)carbodiimide hydrochloride (WSCDI resin, 422 mg, 2.2 mmol) was added to a solution of *t*-Boc-4-aminobutanoic acid (509 mg, 2.2 mmol), 4-amino-4'-nitrodiphenyl sulfide (493 mg, 2.0 mmol), and triethylamine (202 mg, 2.0 mmol) in CH₂Cl₂ (6 ml). After 12 hr stirring at room temperature, the reaction mixture was washed with water, 6 N HCl, water, saturated NaHCO₃ solution, and water. The organic layer was dried over Na₂SO₄ and the solvent evaporated under reduced pressure to give BI-6C12 as a yellow solid (466 mg, 51%). ¹H NMR (*d*-DMSO, 500 MHz): 10.15 (s, 1H), 8.13 (d, *J* = 8.2 Hz, 2H), 7.78 (d, *J* = 5.8 Hz, 2H), 7.55 (d, *J* = 5.8 Hz, 2H), 7.24 (d, *J* = 8.2 Hz, 2H), 2.93–2.91 (m, 2H), 2.35–2.33 (m, 2H), 1.62–1.59 (m, 2H), 1.38 (s, 9H), 1.30–1.25 (m, 4H). ¹³C NMR (*d*-DMSO, 125 MHz): 171.6, 159.4, 155.5, 148.8, 144.7, 141.0, 135.9, 125.9, 124.2, 121.7, 77.2, 36.4, 29.2, 28.2, 25.9, 24.7.

6-Amino-Hexanoic Acid [4-(4-Nitro-Phenylsulfanyl)-Phenyl]-Amide (BI-6D1)

Compound BI-6C12 (460 mg, 1.0 mmol) was added to a round-bottomed flask and cooled to 0°C. The minimum amount of trifluoroacetic acid needed to dissolve the compound was added and the solution let under stirring at room temperature for an additional 5

min. The acid was evaporated at the rotary evaporator and the residue dissolved in CH₂Cl₂. The solution was extracted with a 1 M solution of K₂CO₃ and water. The organic phase was dried over Na₂SO₄ and concentrated under reduced pressure to give the crude BI-6D1 (280 mg, 78%) as a bright yellow solid. The compound was used for the following step with no further purification. ¹H NMR (*d*-DMSO, 500 MHz): 10.16 (s, 1H), 8.13 (d, *J* = 9.0 Hz, 2H), 7.78 (d, *J* = 9.0 Hz, 2H), 7.55 (d, *J* = 8.2 Hz, 2H), 7.24 (d, *J* = 8.2 Hz, 2H), 2.56–2.54 (m, 2H), 2.37–2.36 (m, 2H), 1.63–1.60 (m, 2H), 1.39–1.34 (m, 4H). ¹³C NMR (*d*-DMSO, 125 MHz): 171.7, 148.8, 144.7, 141.1, 135.9, 125.8, 124.2, 123.1, 121.7, 41.4, 36.5, 32.8, 26.0, 24.9.

6-(4-Methoxy-Benzenesulfonylamino)-Hexanoic Acid [4-(4-Nitro-Phenylsulfanyl)-Phenyl]-Amide (BI-6D2)

A suspension of the amine BI-6D1 (280 mg, 0.78 mmol) and triethylamine (132 mg, 1.0 mmol) in 5 ml of CH₂Cl₂ was cooled to 0°C and 4-methoxybenzoyl chloride (177 mg, 0.86 mmol) was added as a solution in 7 ml of CH₂Cl₂. After stirring 2 hr at 0°C and overnight at room temperature, the reaction mixture was washed with water and a saturated solution of NaCl in water. The organic phase was dried over Na₂SO₄ and concentrated under reduced pressure to afford BI-6D2 (368 mg, 90%) as a light yellow solid. ¹H NMR (*d*-DMSO, 500 MHz): 10.14 (s, 1H), 8.13 (d, *J* = 7.8 Hz, 2H), 7.79–7.72 (m, 4H), 7.54 (d, *J* = 8.5 Hz, 2H), 7.23 (d, *J* = 8.5 Hz, 2H), 7.11 (d, *J* = 7.8 Hz, 2H), 3.84 (s, 3H), 2.72–2.70 (m, 2H), 2.33–2.30 (m, 2H), 1.55–1.28 (m, 6H). ¹³C NMR (*d*-DMSO, 125 MHz): 171.5, 161.9, 148.8, 144.7, 141.0, 135.8, 132.1, 125.9, 125.2, 124.1, 123.1, 121.7, 114.2, 55.5, 42.3, 36.3, 28.7, 25.7, 24.5.

6-(4-Methoxy-Benzenesulfonylamino)-Hexanoic Acid [4-(4-Amino-Phenylsulfanyl)-Phenyl]-Amide (BI-6D3)

To a suspension of BI-6D2 (100 mg, 0.19 mmol) in 4 ml of MeOH was added SnCl₂ (213 mg, 0.94 mmol) and the mixture was refluxed for 5 hr. Methanol was then evaporated and a solution of 10% NaHCO₃ was added carefully at 0°C. The residue was extracted with ethyl acetate and the combined organic phases were dried over Na₂SO₄ and concentrated under reduced pressure to give BI-6D3 (80 mg, 84%) as a bright yellow solid. ¹H NMR (*d*-DMSO, 500 MHz): 9.82 (s, 1H), 7.72 (d, *J* = 7.0 Hz, 2H), 7.45 (d, *J* = 7.0 Hz, 2H), 7.38 (bs, 1H), 7.14–7.02 (m, 6H), 6.60 (d, *J* = 10.0 Hz, 2H), 5.42 (bs, 2H), 3.83 (s, 3H), 2.70–2.69 (m, 2H), 2.23 (bs, 2H), 1.51–1.25 (m, 6H). ¹³C NMR (*d*-DMSO, 125 MHz): 170.9, 161.9, 149.5, 137.1, 135.3, 132.7, 132.1, 127.8, 119.7, 116.3, 114.6, 114.4, 114.2, 55.5, 42.3, 36.1, 28.7, 25.7, 24.5.

Experiments with Isolated Mitochondria

100 ng of tBid (cleaved by caspase-8) was preincubated with various concentrations of compounds for 15 min at 30°C in HM buffer (10 mM HEPES, pH 7.4, 250 mM mannitol, 10 mM KCl, 1.5 mM MgCl₂, 1 mM DTT, 1 mM EGTA), then 50 μg of isolated mitochondria from HCT116 cells were added to a final volume of 50 μl in HM buffer. After 1 hr incubation at 30°C, the samples were centrifuged at 10,000 × *g* for 5 min at 4°C and the supernatant was analyzed by SDS-PAGE/immunoblotting using anti-SMAC antibody.

Cell-Based Assays

HEK 293T cells were transfected with 0.5 μg of plasmids encoding either GFP or GFP-tBid in a 12-well plate. After 3 hr transfection, various compounds were added in DMSO to the media. After 20 hr of further incubation, cells were collected and either lysed for caspase assays or fixed and stained with DAPI for determination of apoptosis [50]. For caspase activity assays, 293T cells were lysed in lysis buffer (10 mM HEPES, pH 7.4, 142.2 mM KCl, 5 mM MgCl₂, 0.5 mM EDTD, 0.5% NP-40) containing a protease inhibitor mixture (Roche Molecular Biochemicals). The lysates were normalized for protein concentration (10 μg), then incubated with 100 μM DEVD-AFC. Enzyme activity was determined by the release of AFC fluorescence and V_{max} was calculated (mean ± SD; *n* = 3). For DAPI staining, 293T cells were fixed, washed with PBS, and stained with 0.1 mg/ml DAPI. The percentage of GFP-positive cells with apoptotic morphology (fragment nuclei or condensed chromatin) was determined (mean ± SD; *n* = 3).

Acknowledgments

We thank NIH (CA78040, CA30199-22) and the William R. Hearst Foundation (M.P.) for generous support.

Received: March 30, 2004
Revised: May 19, 2004
Accepted: May 19, 2004
Published: August 20, 2004

References

1. Reed, J.C. (1998). Bcl-2 family proteins. *Oncogene* 17, 3225–3236.
2. Adams, J.M., and Cory, S. (1998). The Bcl-2 protein family: arbiters of cell survival. *Science* 281, 1322–1326.
3. Gross, A., McDonnell, J.M., and Korsmeyer, S.J. (1999). BCL-2 family members and the mitochondria in apoptosis. *Genes Dev.* 13, 1899–1911.
4. Cory, S., and Adams, J.M. (2002). The Bcl2 family: regulators of the cellular life-or-death switch. *Nat. Rev. Cancer* 2, 647–656.
5. Li, H., Zhu, H., Xu, C.J., and Yuan, J. (1998). Cleavage of BID by caspase 8 mediates the mitochondrial damage in the Fas pathway of apoptosis. *Cell* 94, 491–501.
6. Deng, Y., Ren, X., Yang, L., Lin, Y., and Wu, X. (2003). A JNK-dependent pathway is required for TNF α -induced apoptosis. *Cell* 115, 61–70.
7. McDonnell, J.M., Fushman, D., Milliman, C.L., Korsmeyer, S.J., and Cowburn, D. (1999). Solution structure of the proapoptotic molecule BID: a structural basis for apoptotic agonists and antagonists. *Cell* 96, 625–634.
8. Degli Esposti, M. (2002). The roles of Bid. *Apoptosis* 7, 433–440.
9. Gross, A., Yin, X.M., Wang, K., Wei, M.C., Jockel, J., Milliman, C., Erdjument-Bromage, H., Tempst, P., and Korsmeyer, S.J. (1999). Caspase cleaved BID targets mitochondria and is required for cytochrome c release, while BCL-XL prevents this release but not tumor necrosis factor-R1/Fas death. *J. Biol. Chem.* 274, 1156–1163.
10. Brustovetsky, N., Dubinsky, J.M., Antonsson, B., and Jemerson, R. (2003). Two pathways for tBID-induced cytochrome c release from rat brain mitochondria: BAK- versus BAX-dependence. *J. Neurochem.* 84, 196–207.
11. Yin, X.M., Wang, K., Gross, A., Zhao, Y., Zinkel, S., Klocke, B., Roth, K.A., and Korsmeyer, S.J. (1999). Bid-deficient mice are resistant to Fas-induced hepatocellular apoptosis. *Nature* 400, 886–891.
12. Waldmeier, P.C. (2003). Prospects for antiapoptotic drug therapy of neurodegenerative diseases. *Prog. Neuropsychopharmacol. Biol. Psychiatry* 27, 303–321.
13. Guegan, C., Vila, M., Teismann, P., Chen, C., Onteniente, B., Li, M., Friedlander, R.M., Przedborski, S., and Teissman, P. (2002). Instrumental activation of bid by caspase-1 in a transgenic mouse model of ALS. *Mol. Cell. Neurosci.* 20, 553–562.
14. Sattler, M., Liang, H., Nettlesheim, D., Meadows, R.P., Harlan, J.E., Eberstadt, M., Yoon, H.S., Shuker, S.B., Chang, B.S., Minn, A.J., et al. (1997). Structure of Bcl-xL-Bak peptide complex: recognition between regulators of apoptosis. *Science* 275, 983–986.
15. Degterev, A., Lugovskoy, A., Cardone, M., Mulley, B., Wagner, G., Mitchison, T., and Yuan, J. (2001). Identification of small-molecule inhibitors of interaction between the BH3 domain and Bcl-xL. *Nat. Cell Biol.* 3, 173–182.
16. Tzung, S.P., Kim, K.M., Basanez, G., Giedt, C.D., Simon, J., Zimmerberg, J., Zhang, K.Y., and Hockenbery, D.M. (2001). Antimycin A mimics a cell-death-inducing Bcl-2 homology domain 3. *Nat. Cell Biol.* 3, 183–191.
17. Kitada, S., Leone, M., Sareth, S., Zhai, D., Reed, J.C., and Pellecchia, M. (2003). Discovery, characterization and structure-activity relationships studies of pro-apoptotic polyphenols targeting Bcl-xL. *J. Med. Chem.* 46, 4259–4264.
18. Leone, M., Zhai, D., Sareth, S., Kitada, S., Reed, J.C., and Pellecchia, M. (2003). Cancer prevention by tea polyphenols is linked to their direct inhibition of antiapoptotic Bcl-2-family proteins. *Cancer Res.* 63, 8118–8121.
19. Becattini, B., Kitada, S., Leone, M., Monosov, E., Chandler, S., Zhai, D., Kipps, T.J., Reed, J.C., and Pellecchia, M. (2004). Rational design and real time in-cell detection of the proapoptotic activity of a novel compound targeting Bcl-XL. *Chem. Biol.* 11, 389–395.
20. Huang, Z. (2002). The chemical biology of apoptosis. Exploring protein-protein interactions and the life and death of cells with small molecules. *Chem. Biol.* 9, 1059–1072.
21. O'Neill, J.W., and Hockenbery, D.M. (2003). Bcl-2-related proteins as drug targets. *Curr. Med. Chem.* 10, 1553–1562.
22. Osford, S.M., Dallman, C.L., Johnson, P.W., Ganesan, A., and Packham, G. (2004). Current strategies to target the anti-apoptotic Bcl-2 protein in cancer cells. *Curr. Med. Chem.* 11, 1031–1039.
23. Chou, J.J., Li, H., Salvesen, G.S., Yuan, J., and Wagner, G. (1999). Solution structure of BID, an intracellular amplifier of apoptotic signaling. *Cell* 96, 615–624.
24. Fejzo, J., Lepre, C.A., Peng, J.W., Bemis, G.W., Ajay, Murcko, M.A., and Moore, J.M. (1999). The SHAPES strategy: an NMR-based approach for lead generation in drug discovery. *Chem. Biol.* 6, 755–769.
25. Shuker, S.B., Hajduk, P.J., Meadows, R.P., and Fesik, S.W. (1996). Discovering high-affinity ligands for proteins: SAR by NMR. *Science* 274, 1531–1534.
26. Bemis, G.W., and Murcko, M.A. (1996). The properties of known drugs. 1. Molecular frameworks. *J. Med. Chem.* 39, 2887–2893.
27. Pellecchia, M., Sem, D.S., and Wuthrich, K. (2002). NMR in drug discovery. *Nat. Rev. Drug Discov.* 1, 211–219.
28. Ni, F. (1994). Recent developments in transferred NOEs methods. *Prog. Nucleic Magn. Reson. Spectrosc.* 26, 517–606.
29. Mayer, M., and Meyer, B. (2000). Mapping the active site of angiotensin-converting enzyme by transferred NOE spectroscopy. *J. Med. Chem.* 43, 2093–2099.
30. Kumar, A., Ernst, R.R., and Wuthrich, K. (1980). A two-dimensional nuclear Overhauser enhancement (2D NOE) experiment for the elucidation of complete proton-proton cross-relaxation networks in biological macromolecules. *Biochem. Biophys. Res. Commun.* 95, 1–6.
31. Jahnke, W., Florsheimer, A., Blommers, M.J., Paris, C.G., Heim, J., Nalin, C.M., and Perez, L.B. (2003). Second-site NMR screening and linker design. *Curr. Top. Med. Chem.* 3, 69–80.
32. Li, D., DeRose, E.F., and London, R.E. (1999). The inter-ligand Overhauser effect: a powerful new NMR approach for mapping structural relationships of macromolecular ligands. *J. Biomol. NMR* 15, 71–76.
33. Pellecchia, M., Meininger, D., Dong, Q., Chang, E., Jack, R., and Sem, D.S. (2002). NMR-based structural characterization of large protein-ligand interactions. *J. Biomol. NMR* 22, 165–173.
34. Zerbe, O. (2003). *BioNMR in Drug Research* (Weinheim, Germany: Wiley-VCH).
35. Kline, A. (1997). SAR by NOE? *The NMR Newsletter* 13, 472.
36. Pervushin, K., Riek, R., Wider, G., and Wuthrich, K. (1997). Attenuated T2 relaxation by mutual cancellation of dipole-dipole coupling and chemical shift anisotropy indicates an avenue to NMR structures of very large biological macromolecules in solution. *Proc. Natl. Acad. Sci. USA* 94, 12366–12371.
37. Kramer, B., Rarey, M., and Lengauer, T. (1999). Evaluation of the FLEX incremental construction algorithm for protein-ligand docking. *Proteins* 37, 228–241.
38. Sheehan, J.C., Preston, J., and Cruickshank, P.A. (1965). A rapid synthesis of oligopeptide derivatives without isolation of intermediates. *J. Am. Chem. Soc.* 87, 2492–2493.
39. Kamal, A., Ramesh, G., Laxman, N., Ramulu, P., Srinivas, O., Neelima, K., Kondapi, A.K., Sreenu, V.B., and Nagarajaram, H.A. (2002). Design, synthesis, and evaluation of new noncross-linking pyrrolobenzodiazepine dimers with efficient DNA binding ability and potent antitumor activity. *J. Med. Chem.* 45, 4679–4688.
40. Korsmeyer, S.J., Wei, M.C., Saito, M., Weiler, S., Oh, K.J., and Schlesinger, P.H. (2000). Pro-apoptotic cascade activates BID, which oligomerizes BAK or BAX into pores that result in the release of cytochrome c. *Cell Death Differ.* 7, 1166–1173.

41. Lynden, P., and Wahlgren, N.G. (2000). Mechanisms of action of neuroprotectants in stroke. *J. Stroke Cerebravasc. Dis.* **9**, 9–14.
42. Friedlander, R.M. (2003). Apoptosis and caspases in neurodegenerative diseases. *N. Engl. J. Med.* **348**, 1365–1375.
43. Li, D., Levy, L.A., Gabel, S.A., Lebetkin, M.S., DeRose, E.F., Wall, M.J., Howell, E.E., and London, R.E. (2001). Interligand Overhauser effects in type II dihydrofolate reductase. *Biochemistry* **40**, 4242–4252.
44. Wei, M.C., Lindsten, T., Mootha, V.K., Weiler, S., Gross, A., Ashiya, M., Thompson, C.B., and Korsmeyer, S.J. (2000). tBID, a membrane-targeted death ligand, oligomerizes BAK to release cytochrome c. *Genes Dev.* **14**, 2060–2071.
45. Chittenden, T. (2002). BH3 domains: intracellular death-ligands critical for initiating apoptosis. *Cancer Cell* **2**, 165–166.
46. Scorrano, L., and Korsmeyer, S.J. (2003). Mechanisms of cytochrome c release by proapoptotic BCL-2 family members. *Biochem. Biophys. Res. Commun.* **304**, 437–444.
47. Schendel, S.L., Azimov, R., Pawlowski, K., Godzik, A., Kagan, B.L., and Reed, J.C. (1999). Ion channel activity of the BH3 only Bcl-2 family member, BID. *J. Biol. Chem.* **274**, 21932–21936.
48. Clark, R.D., Strizhev, A., Leonard, J.M., Blake, J.F., and Matthew, J.B. (2002). Consensus scoring for ligand/protein interactions. *J. Mol. Graph. Model.* **20**, 281–295.
49. Teschner, M., Henn, C., Vollhardt, H., Reiling, S., and Brickmann, J. (1994). Texture mapping: a new tool for molecular graphics. *J. Mol. Graph.* **12**, 98–105.
50. Zhai, D., Ke, N., Zhang, H., Ladrer, U., Joseph, M., Eichinger, A., Godzik, A., Ng, S.C., and Reed, J.C. (2003). Characterization of the anti-apoptotic mechanism of Bcl-B. *Biochem. J.* **376**, 229–236.